Available online at www.sciencedirect.com
SCIENCE DIRECT
Environmental Pollution 141 (2006) 295–309
ENVIRONMENTAL POLLUTION
www.elsevier.com/locate/envpol

Natural and anthropogenic geochemical signatures of floodplain and deltaic sedimentary strata, Sacramento–San Joaquin Delta, California, USA

G.B. Pasternack [a,*], K.J. Brown [a,b]

[a] Department of Land, Air and Water Resources, University of California, 211 Veihmeyer Hall, One Shields Avenue, Davis, CA 95616-8628, USA
[b] Department of Quaternary Geology, Geological Survey of Denmark and Greenland, Øster Voldgade 10, DK-1350 Copenhagen K, Denmark

Received 25 January 2005; accepted 8 August 2005

Geomorphic–geochemical linkages on an upper deltaic plain have dynamics that defy expectations for achieving restoration ''success''.

Abstract

The geochemical history of an upper deltaic plain pending tidal wetland restoration was reconstructed to assess remobilization of redox-sensitive constituents in sediment, identify depositional processes promoting geochemical retention, and determine the extent of contamination with Hg, As, Pb, Cu, and Zn. Three 12–14-m sediment cores were analyzed for bulk sediment geochemistry using ICP-AES. Rather than showing similar stratigraphic and geochemical down-core trends, cores had a unique record indicative of strong spatial gradients in deposition processes. Each strata type (e.g. basal clay, sand channel, distal floodplain, and agriculturally impacted surficial horizon) had a unique geochemical ''fingerprint''. The agriculturally impacted surficial layer showed high [Hg], [As], and [Pb]. The significance is that a restored upper delta will have a complex geomorphology defying conventional criteria of ''success'' in a restoration framework. Also, there is a significant risk of generating toxic, bio-available CH_3Hg^+ that would be hazardous to fish.

Keywords: Metal accumulation; Wetland restoration; Deltas; Sedimentation; Trace metals

1. Introduction

Upper deltaic plains present a unique and challenging environment for assessment of geomorphic, stratigraphic, and geochemical processes. Because of their landscape position in the tidal freshwater zone, they are subjected to a complex array of physical and chemical coastal or estuarine (i.e. receiving basin) as well as watershed (i.e. contributing basin) processes acting over a wide range of human-relevant timescales (Pasternack, 1998). With regard to hydrological and associated processes that occur on hourly to weekly timescales, such systems are commonly dominated by receiving basin dynamics related to tides and/or winds (Pasternack and Hinnov, 2003). These processes are often visible to environmental managers and thus are highly emphasized in planning. In contrast, contributing basin dynamics, such as land use change, infrequent floods, geomorphic adjustments, and sediment yield, operate on decadal to centennial timescales (Pasternack et al., 2001; Brown and Pasternack, 2004). These dynamics control the longevity and sustainability of environmental management activities, but their influence can only be discerned through thorough analysis of longer-term records, such as sediment cores, historic maps, or rare long-term datasets.

In general, deltas are often characterized as having a two-fold history comprising a constructional phase followed by a destructive phase (Elliot, 1986). Human activities can enhance

* Corresponding author. Tel.: +1 530 754 9243; fax: +1 530 752 5262.
E-mail address: gpast@ucdavis.edu (G.B. Pasternack).

0269-7491/$ - see front matter © 2005 Elsevier Ltd. All rights reserved.
doi:10.1016/j.envpol.2005.08.044

or alter these phases (Pasternack et al., 2001), confounding prediction of future conditions. Delta morphology generally consists of three zones, namely deltaic plains (subaerial), the delta front (subaqueous), and the prodelta (deep water). Colman (1976) termed the ''upper deltaic plain'' as the region above significant tidal or marine influence that is dominated by riverine depositional processes. Given this position at the head of a delta, upper deltaic plains may additionally experience a complex combination of non-tidal floodplain processes as well as tidally influenced delta processes. Goodbred and Kuehl (1998) reported that the upper deltaic plain of the Brahmaputra-Ganges system included significant areas of inactive floodplain isolated by channel avulsion.

In terms of geochemistry, deltas may act as sinks or sources for rock-derived constituents (e.g. Al, Fe, Ca, Mg, Na, and K) and human-generated pollutants (e.g. Hg, Pb, As, Cd, Cu, Zn, Ni), depending on the dominant hydrogeomorphic processes and anthropogenic influences. Accumulation and retention occur both by sediment deposition and solute transport. The former encompasses input and burial of metals already incorporated into fine inorganic and organic particles (Warren, 1981; Olsen et al., 1982; Olsenholler, 1991). Along urbanized coasts, direct runoff and tidally redistributed urban pollution can significantly contribute to metal accumulation in deltaic soils (Velinsky et al., 1994; Knight and Pasternack, 2000). Solute transport mechanisms, on the other hand, involve adsorption of metals onto soil and decomposing plant litter (Millward and Moore, 1982; Simpson et al., 1983a, b; Orson et al., 1992), downward migration of free metals into sedimentary strata (Simpson et al., 1983b; Dubinski et al., 1986), and plant uptake (Sculthorpe, 1967; Banus et al., 1975; Dowdy and Larson, 1975). Conversely, sediment erosion and export can occur by wind-wave attack (Pasternack, 1998), overbank flooding and scouring of the delta plain as occurs on floodplains (Florsheim and Mount, 2002), and by channel incision. Solute-based losses can occur over longer periods of time via diagenesis and re-mobilization of easily dissolved constituents (Hudson-Edwards et al., 1998).

In this study conducted in northern California, USA, the centennial to millennial coupling between geomorphic and geochemical dynamics occurring in an upper deltaic plain was investigated through interdisciplinary analyses of three long (10–15 m) sediment cores. Specifically, we sought to (a) assess the degree of remobilization of redox-sensitive chemical constituents (e.g. S, Fe, Mn, Cu, Zn) over centuries to millennia as a function of strata type, (b) identify the depositional processes that promote geochemical retention of different constituents (e.g. basin-derived flooding, tidal inundation, peat formation, and natural levee breaching), and (c) determine the extent that the upper deltaic plain traps and retains rock-derived and human-generated elemental pollutants, specifically Hg, As, Pb, Cu, and Zn. Although this study delineates the natural versus anthropogenic geochemical conditions in the upper deltaic plain of the Sacramento-San Joaquin delta, the geomorphic conditions associated with this zone turned out to be too complex and disturbed by land use to provide a detailed post-European settlement geochemical history.

2. Study area

The Sacramento-San Joaquin Delta is a large (299,000 ha) tidal delta located inland of San Francisco Bay in central California. The drainage basin feeding the delta is extensive, covering $\sim$107,000 km^2 from northern to southern California (Fig. 1). The annual outflow of water through the delta is $\sim$19 billion m^3. The delta is dominated by sediment input, with annual in- and out-fluxes of $\sim$4.7 and $\sim$3.3 million metric tons of suspended sediment, respectively (Galloway, 1975; Conomos and Peterson, 1976). The lower delta plain shows some morphological influence of winds and mixed tides. Winds typically blow towards the east at an average speed of 2–5 m s^{-1} with gusts peaking at 15–21 m s^{-1} (Conomos and Peterson, 1976). The summer tidal range at the seaward end of the delta is $\sim$1.4 m whereas that in upper delta distributary channels $\sim$1.0 m. The delta has a rejoining distributary channel pattern (sensu Colman, 1976) because of erratic discharges and the high tidal range. Extensive levee construction and maintenance over the past 150 years has enabled widespread agricultural activity in the delta, presently accounting for $\sim$73% of the delta's area (Logan, 1990).

The Sacramento–San Joaquin Delta has been subjected to an extremely high influx of Hg as a result of historic Hg and Au mining in California in the late 19th century. Hg mining in the Coastal Range northwest of the delta supplied Hg directly to the delta through connecting streams (e.g. Cache Creek). Additional Hg was added to the delta through its translocation and use in Au mining in the Sierra Nevada northeast, east, and southeast of the delta. Many studies have recently been performed to characterize the Hg in the organisms (e.g. Choi et al., 1998; Cain et al., 2000), water (e.g. Choe et al., 2003), and sediment (e.g. Domagalski, 1998, 2001) of the delta and associated waterways. For reference in this study, total [Hg] in Sacramento basin river-bed material is 50–400 ppb whereas in Sacramento Valley sloughs it is 30–90 ppb (Domagalski, 2001). Of these totals, measurements found up to 8% actually reactive to reducing conditions, becoming toxic CH_3Hg^+ (Domagalski, 2001), though toxicity effects on organisms were not studied. Reactivity of high [Hg] waters and sediments was inhibited when the constituent was in the mercury sulfide form.

The McCormack–Williamson Tract (MWT) is uniquely located at the head of the Sacramento-San Joaquin Delta, downstream from the confluence of the Cosumnes and Mokelumne rivers and adjacent to the Sacramento River (Fig. 1). The Cosumnes River is the only major river flowing out of the Sierra Nevada whose mainstem is not dammed. MWT is $\sim$650 ha in area and is bordered by the Mokelumne River to the east, Snodgrass Slough to the west, and artificial dredge channels to the north and northeast. Climate is Mediterranean, with cool, wet winters and hot, dry summers. Average monthly temperatures range from $\sim$2 °C in December to 33 °C in July, while average monthly rainfall varies from $\sim$2 mm in July to 80 mm in January. Annual precipitation is $\sim$430 mm. Spring snowmelt from the Sierra Nevada is now detained in reservoirs, but historically it created widespread lowland

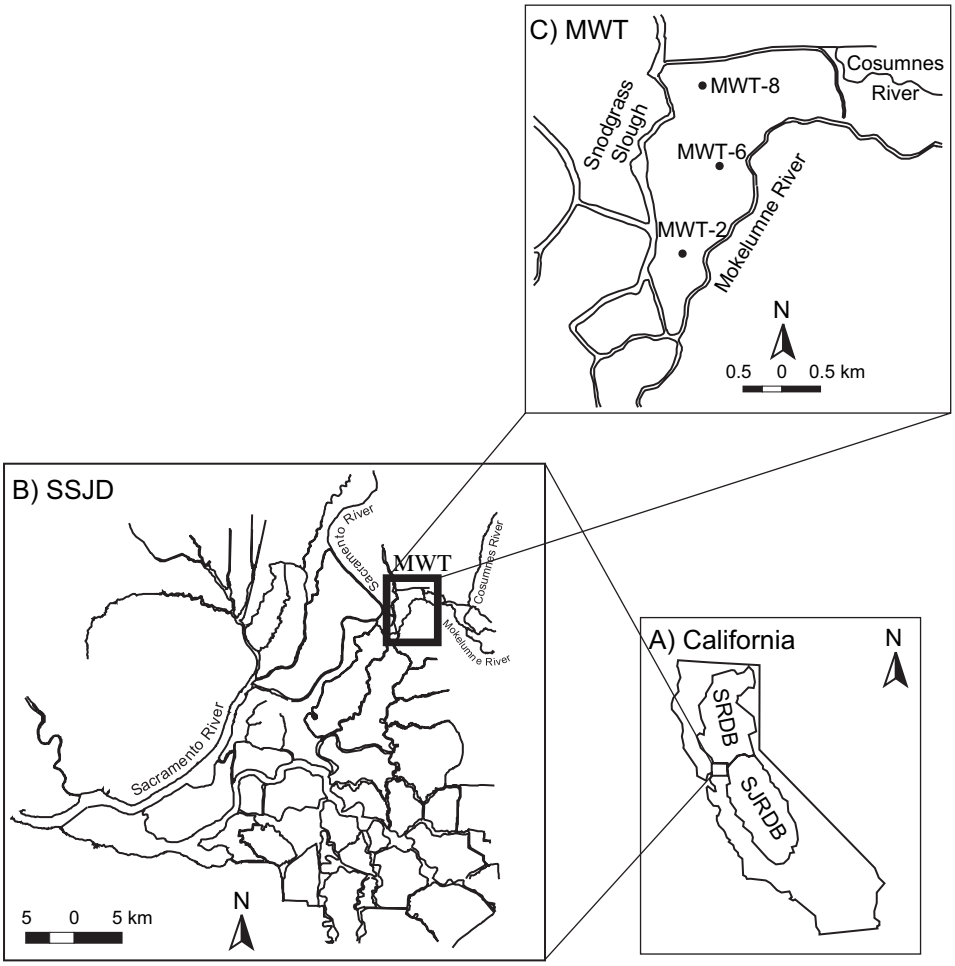

Fig. 1. (A) Sacramento (SRDB) and San Joaquin (SJRDB) river drainage basins within California. The box shows the position of the Sacramento–San Joaquin Delta (SSJD). (B) Map of the SSJD showing the relative position (box) of the McCormack–Williamson Tract (MWT) at the head of the delta in relation to major rivers. (C) Map of MWT showing where 3 deep cores were collected.

flooding that now only occurs during extremely wet years or during a rain-on-snow event.

Historic maps show that MWT was a freshwater wetland in the early 20th century (United States Geological Survey, 1911). The wetland was likely tidal, as the adjacent modern channels are presently tidal for several kilometers upstream from the site. Subsequently, the tract was leveed, drained, and converted into agricultural land. After drainage, MWT and other delta islands experienced subsidence as surface organic sediment was oxidized and decomposed (Rojstaczer et al., 1991). The little riparian vegetation that exists at MWT is found on the levees. Because of its unique landscape position, wetland restoration is planned for MWT. The potential benefits of MWT restoration include increased biodiversity, increased waterfowl and native fish habitat, improved water quality, and flood-damage mitigation.

3. Methods

3.1. Core retrieval and processing

To characterize past geochemical conditions at MWT, three 12–14-m long sediment cores (MWT-2, MWT-6, and MWT-8) were collected along the longitudinal axis of the tract (Fig. 1). MWT-2 is located near the southern tip where the elevation is −30 cm relative to the 1929 National Geodetic Vertical Datum (NGVD) mean sea level position. MWT-6 is centrally located on MWT and is +30 cm NGVD. MWT-8 is located in the northwest section of MWT and is also +30 cm NGVD.

The 5-cm diameter cores were collected incrementally using a Geoprobe drilling rig with direct push and dual-tube sampling technology that enabled the cores to be recovered in 1.22-m long plastic liners. Sediment compaction or expansion during coring was measured on a section-by-section basis as the difference between pushed distance and actual core length. Core sections were temporarily stored vertically in a refrigerated room at ~4 °C. Core liners were first cut lengthwise using a circular saw on opposite sides and then a nylon string was passed through the core center to yield two sediment halves. Any smeared material was carefully scrapped off the exposed sediment surface in a horizontal fashion using a plastic spatula. Subsequently, stratigraphy and lithology of each core was assessed using magnetic susceptibility, digital photography, and visual assessment (Brown and Pasternack, 2004). Cores were then subsampled in 10-cm intervals.

Subsamples were placed in labeled plastic bags, refrigerated at ~4 °C, and later analyzed.

AMS radiocarbon dating and quantitative stratigraphic analyses at 10-cm resolution were previously performed as detailed in Brown and Pasternack (2004). Non-linear radiocarbon and calendar year age-depth models were developed by fitting locally weighted functions to the reported dates. Radiocarbon dating is the most suitable and preferred radionuclide dating technique for the millennial time interval being examining. Pb-210 and Cs-137 analysis only reveal 120-year and 55-year ranges, and were not undertaken because the surface agricultural layer has been mixed by tilling, thus rendering any emergent chronologies from these methods unclear and imprecise. Pollen was not consistently preserved among strata for use in sediment dating, though agricultural and disturbance grains such as maize and Chenopodiaceae were observed in the agricultural horizon. Sediment characteristics such as bulk density, grain size distributions (with separation of fines versus sands by wet sieving), loss-on-ignition (LOI), and magnetic susceptibility were measured for all core subsamples. Vertical accretion (cm $year^{-1}$), sedimentation rates (g cm^{-2} $year^{-1}$), and chemical loadings (mg cm^{-2} $year^{-1}$) were determined using the established calendar age-depth models.

3.2. Chemical analysis

Determination of the leachable elemental concentrations of every other sample (i.e. 20-cm resolution) was carried out by ALS Chemex of Sparks, Nevada using accepted standard methods. The procedure involved first air drying the samples and sieving them through a #80 mesh (<0.177 mm), the standard size used in soil geochemical characterization. Samples were then well mixed and treated with hot concentrated nitric acid to destroy organic matter and oxidize sulfide material. Addition of concentrated hydrochloric acid (3 times the volume of the nitric acid) to the sample generated an aqua regia ($3\ HCl + HNO_3 = 2\ H_2O + NOCl + Cl_2$) that was used to leach the material. After leaching, sample solutions were analyzed by inductively coupled argon plasma and atomic emission spectroscopy to obtain the concentrations of 33 elements (Ag, Al, As, B, Ba, Be, Bi, Ca, Cd, Co, Cr, Cu, Fe, Ga, K, La, Mg, Mn, Mo, Na, Ni, P, Pb, S, Sb, Sc, Sr, Ti, Tl, U, V, W, Zn). [Hg] was determined by cold volatilization atomic adsorption spectroscopy. Detection limits for the primary elements used in the study are given in Table 1. Full details on analytical methods are available at http://www.alschemex.com.

The Quality Assurance program at ALS Chemex (ISO 9001:2000 registration) is a multi-level program involving clearly defined quality control procedures for sample preparation and analysis, plus a quality assessment stage that includes data review and statistical analysis. Standard operating procedures including use of reference materials, duplicates, and blanks were performed. In the event that any reference material or duplicate result fell outside the established control limits, an Error Report was automatically generated and an investigation performed. A QA/QC report is available with the Certificate of Analysis obtained on the samples assayed for this study. Full details on all preparation and analysis QA/QC protocols are available at http://www.alschemex.com.

Table 1
Elemental abundances in a NIST reference sample assayed by partial leaching (Chemex) and by total digestion (NIST) sorted by leaching percent with lower detection limit indicated

Element	Units	Limit	Chemex	NIST	Leach (%)
Ag	ppm	0.01	0.6	0.41	146
As	ppm	0.1	18	17.7	102
Cd	ppm	0.01	<0.5	0.38	bd
Cu	ppm	0.2	33	34.6	95
S	%	0.01	0.08	0.089	90
Co	ppm	0.1	12	13.4	90
P	ppm	10	530	620	85
Ni	ppm	0.2	75	88	85
Zn	ppm	2	90	106	85
Mn	ppm	5	445	538	83
Fe	%	0.01	2.86	3.5	82
Mg	%	0.01	1.22	1.51	81
Ca	%	0.01	1.41	1.89	75
Hg	ppb	10	1040	1400	74
Pb	ppm	0.2	10	18.9	53
Mo	ppm	0.05	1	2	50
Sr	ppm	0.2	111	231	48
V	ppm	1	52	112	46
Cr	ppm	1	55	130	42
Sc	ppm	0.1	5	12	42
Ba	ppm	0.2	380	968	39
Al	%	0.01	2.05	7.5	27
K	%	0.01	0.3	2.03	15
Ti	%	0.02	0.03	0.342	9
Na	%	0.01	0.07	1.16	6

bd, below detection limit.

Because sediment digestion was ''total'' for most base metal sulfates, sulfides, oxides and carbonates, but only ''partial'' for most rock-forming and refractory elements, a local reference soil sample whose total composition is well known was obtained from the National Institute of Standards and Technology (San Joaquin Soil Standard Reference Material 2709) and analyzed using the same chemical procedure as for the study samples. The difference between the measured and known element concentrations for the reference standard was the non-leachable fraction. Because the reference material came from a field close to the study site, its texture, composition, and thus leachable fraction should be very similar to those for samples from the sediment cores. Other than Al, elements showing very poor leaching (<50%) or with concentrations close to the minimum detection limit were excluded from further analysis. These were Ag, B, Ba, Be, Cd, Ga, K, La, Mo, Na, Sb, Sc, Ti, Tl, U, V, W.

Among poorly leached constituents, those fractions present in fine-grained secondary mineral precipitates would be most available for leaching. Some Al may have been thus available in this form, but most Al in sediment is locked in acid-resistant primary aluminosilicate minerals and hence stable throughout the leaching process. Thus, Al was expected to have a low recovery through leaching, as observed in other wetland sediments (Knight and Pasternack, 2000). Wetland sediments inevitably experience differential leaching with corresponding differences in [Al] (Loring, 1991). To account for this artifact

of the geochemistry procedure used, binary correlations between Al and all other elements were computed. Concentrations of all elements showing a strong relation with Al were normalized by [Al] to remove the effect of leaching. This is viewed as superior to simple correction using the leaching percentages from the NIST reference, because the overall composition may vary substantially from sample to sample and the Al correction accounts for this variation whereas the NIST leaching percentages do not.

Chemical analyses were performed on sieved, air-dried, well-mixed samples containing varying levels of organic material. Because organic content strongly relates to fine sediment content and the latter also relates to degree of leaching, it might have been difficult to distinguish whether changes in concentration down-core were due to binding to organic matter or differential leaching. However, the organic content of core strata derives from two distinct sources- a landscape-derived wash load fraction composed of only 0–7% organic matter and an in situ, peaty wetland-derived fraction composed of 15–32% organic matter (Brown and Pasternack, 2004). The geochemistry of these two sources is unknown. The wash load fraction is in a low abundance directly proportional to fine-sediment abundance. Because significant binding would be limited to peaty strata with more abundant organic matter, organic binding was assessed by observing any significant increase in elemental concentration in peat layers relative to non-peat layers. Elements showing no peak in concentration in peat strata were assumed to stem from the inorganic fraction, so their concentrations were adjusted to an organic-free basis by dividing each raw concentration by the fraction of the total sample that was inorganic. Since inorganic fractions in non-peaty strata were 0.93–1.0, these were minor adjustments.

3.3. Data analysis

Chemical compositions were analyzed to assess inter-elemental sediment geochemistry, down-core strata-averaged trends in concentrations, and cross-core geochemical patterns. Standard approaches were used to investigate inter-elemental sediment geochemistry (Loring, 1991; Knight and Pasternack, 2000). A binary correlation matrix was computed for each core to check for high correlations among elements indicative of binding onto organics, carbonates, Mn-oxides, and Fe-oxides. Principal components analysis (PCA) was also used to segregate variables into groups according to their related chemical functionality for two datasets: (a) raw concentrations for all elements and (b) a mix of raw and Al-normalized concentrations as dictated by each element's leaching effectiveness. Since each concentration is its own variable, and all samples have values for all variables, there is no problem with mixing variables of different units and non-dimensional variables. The results of PCA include percent of variation explained, communalities, loadings, and rotated loadings (using the ''varimax normalized approach'' [e.g. Varekamp et al., 2000]).

The degree of remobilization of individual constituents was assessed by identifying strata presumed to have distinct redox conditions (since they were not measured) and then comparing the abundances of individual constituents with the same units (e.g. $[S]_{strata1}$ vs. $[S]_{strata2}$) between these strata and others. Redox conditions at MWT were hypothesized to vary as a function of hydrogeomorphic conditions, with strongly oxidizing conditions associated with well-drained sand channel units and strongly reducing conditions associated with peaty wetland units. It was hypothesized that remobilized constituents would be trapped in peaty wetland units, yielding significantly higher concentrations in such strata.

Down-core trends were examined to assess the relation between geomorphic units representative of distinct depositional processes and geochemistry. To do this, the stratigraphically constrained cluster zonation of Brown and Pasternack (2004) based on LOI, fine sediment (clay and silt) percentage, magnetic susceptibility, and leachable Al abundance was used to divide the core into distinct units. The average concentration or Al-normalized concentration of well-leached constituents was calculated. Finally, these values were sorted in order of abundance and plotted, with a line for each strata.

Cross-core comparisons were done using two methods to assess the spatial pattern of the observed geochemistry. First, cross-core strata-averaged abundances were computed for each strata type to test the hypothesis that spatial patterns in chemistry more strongly reflect strata type than absolute depth. Second, as a basis for comparison to the strata-averaged cross-core patterns, elemental abundances were considered as a function of depth and time by plotting selected elements for all three cores as a function of depth and time on a single plot to assess temporal cross-correlations independent of stratigraphy. The plots were assessed for peaks indicative of key events or long-term trends related to climate variation, human activities, or landform changes. Selective elements were plotted as a function of time for all three cores on a single plot to assess cross-core patterns. Concentrations associated with distinct geomorphic units were calculated and compared across units.

4. Results

Based on the NIST reference sediment from a nearby field, many elements showed excellent recoveries (Table 1). The only important elements that were very poorly leached were Na and K. Ag was the only element significantly overestimated, likely because it was near the lower detection limit or potentially due to contamination, so it was excluded from further analysis. Sr, Ba and Cr did not leach well, but were further investigated to some extent using caution. Recoveries of Cu and Zn were notably better than previous studies (e.g. Velinsky et al., 1994; Knight and Pasternack, 2000), but varied widely for each constituent. The key to further analysis was identification of a low-recovery element whose variation in concentration would reflect differences in leachate strength and grain size effects.

4.1. Inter-element sediment geochemistry

Aluminum was found to behave as a master variable controlling the first-order variations in several elements due to

differential leaching and its grain size response, as expected. Using the previous results from Brown and Pasternack (2004), [Al] closely tracked fine sediment content (<63 μm) for all cores, which varies strongly as a function of depth in MWT-2 and MWT-6 (Fig. 2). Even though samples were sieved to exclude coarse sediment prior to chemical leaching, this trend suggests that some of the differences in metal extraction could be due to grain size variations at the sub-177 μm level. When Fe, Ca, Mg, Cu, and Zn were plotted against Al, they showed a strong direct linear response to Al for all cores (Fig. 3). Table 2 shows the R^2-values for all elements, with any value above 0.26 statistically significant above the 95% confidence level (values in bold). In contrast, when Fe was correlated with other variables, much poorer relations were found, contravening the basis for normalization. Key elements that were not influenced by Al were Mn, S, P, Hg, Pb, and As. Ni and Co showed a mixed response and were investigated with and without normalization.

Al-normalized elements were compared against each other using a correlation matrix and binary regressions (Table 3, Fig. 4). No cross-core consistent evidence for Fe_xO_y or $CaCO_3$ binding of Mg, Cu, or Zn was evident. MWT-6 alone showed a strong role for Fe_xO_y binding (Fig. 4b,e). Zn/Cu ratios were 1.55, 2, and 1.65 for MWT-2, MWT-6, and MWT-8, respectively. These ratios are much lower than commonly observed in wetlands (~4). The difference appears to be due to higher than normal Cu and slightly lower Zn. These ratios occur throughout all core depths, so differential diagenesis is precluded.

MWT-8 was the only core containing peaty layers with plant fragments and organic content >10%. When the concentration or Al-normalized abundance of each element present in peaty

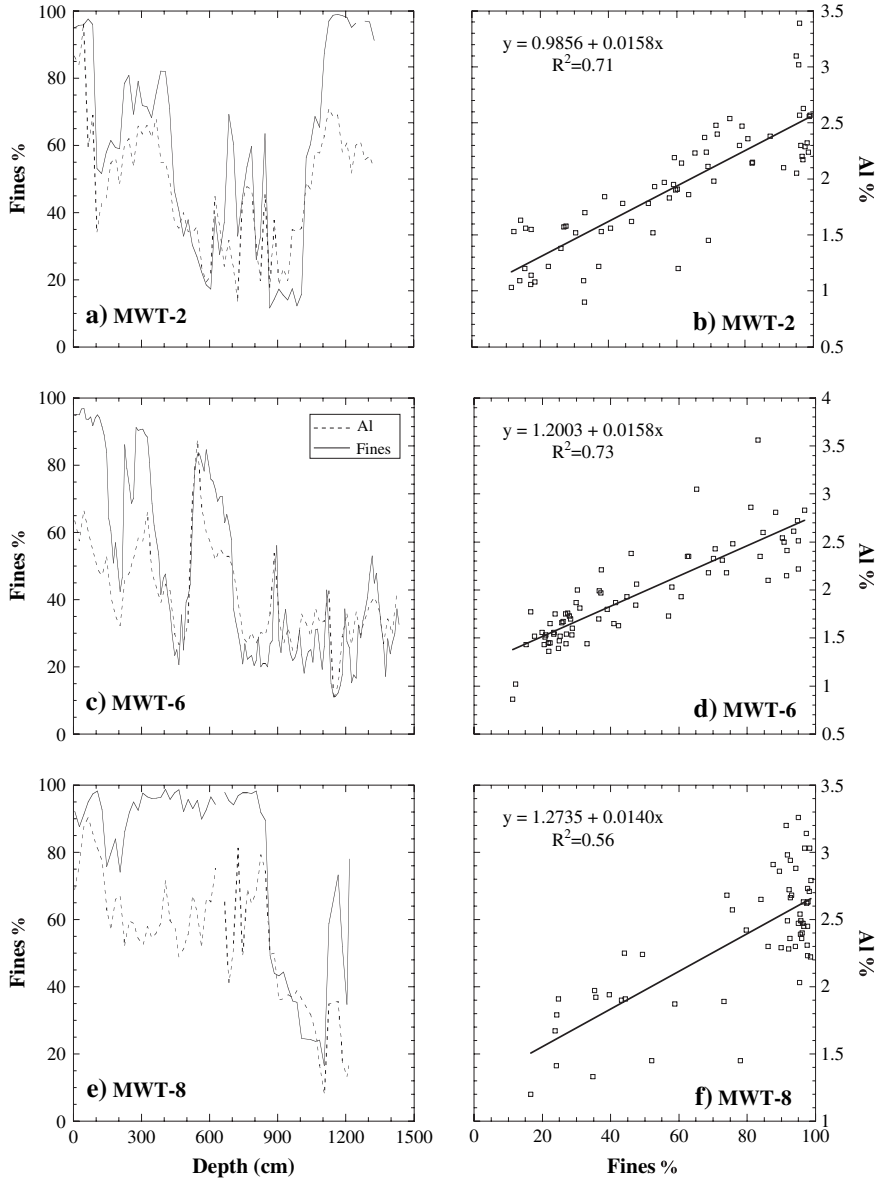

Fig. 2. Relations between Al concentration and fine sediment content (<63 μm) for every other 10-cm sample down-core for MWT-2 (a,b), MWT-6 (c,d), and MWT-8 (e,f). Second *Y*-axis for [Al] applies to both types of plots. All relations were significant above the 95% confidence level.

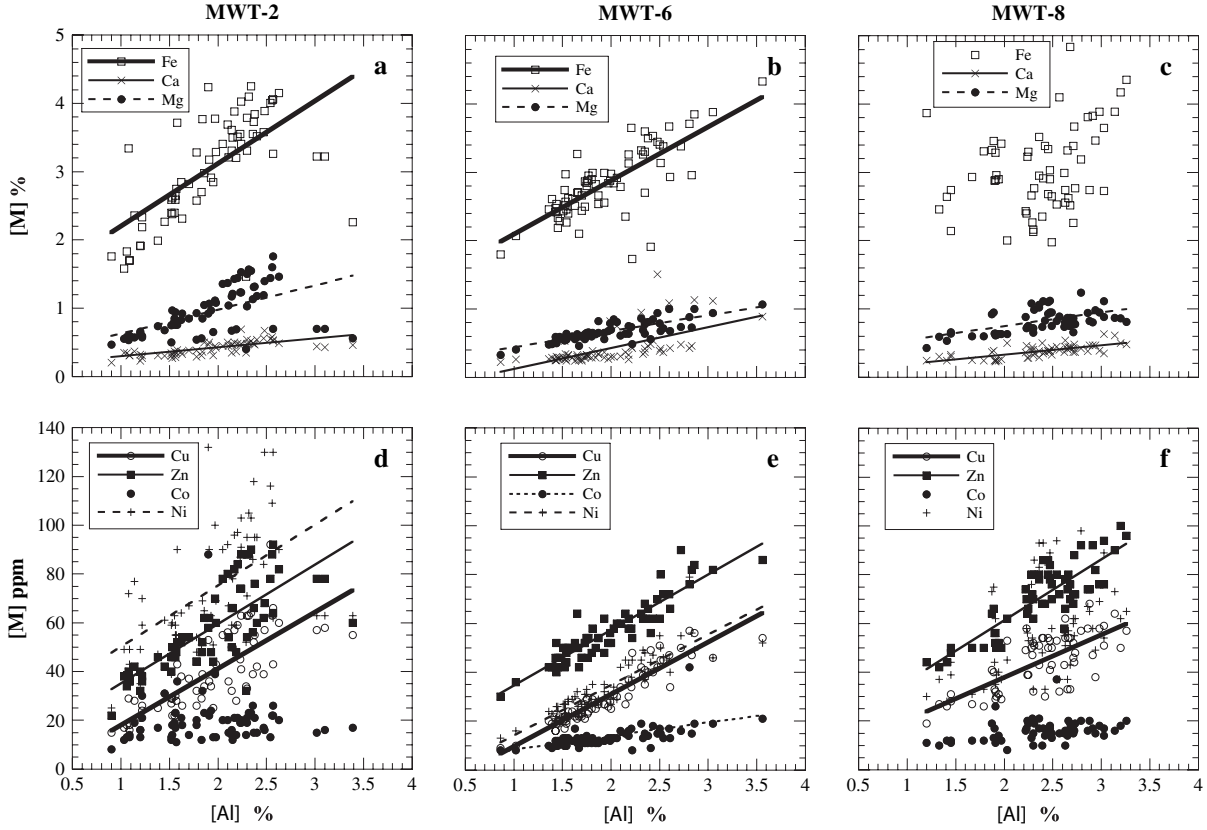

Fig. 3. Relations between Al concentration and other elements for every other 10-cm sample down-core for MWT-2 (a,d), MWT-6 (b,e), and MWT-8 (c,f). Regression lines are shown for statistically significant relations at the 95% confidence level, which indicates partial leaching of those constituents.

strata was averaged and compared against the average of those values for inorganic-dominated strata, only S showed a significant difference. Average extracted [S] in peaty layers was 0.23% whereas that in inorganic-dominated strata was 0.04%. The high abundance of decaying organic material and S together suggests a reducing redox state that might affect the remobilization of elements, because as organic matter decomposes, it consumes any available oxygen, leaving S in a reduced state. No other elements showed significant deviations in the peaty strata relative to the inorganic-dominated layers.

Table 2
R^2 values for relation between each element and Al

Element	MWT-2	MWT-6	MWT-8
Fe	**0.41**	**0.58**	0.11
Ca	**0.43**	**0.39**	**0.51**
Mg	**0.29**	**0.68**	**0.33**
Mn	0.02	**0.38**	**0.44**
S	0.01	0.01	0.02
P	0.14	0.02	0.24
Cu	**0.62**	**0.88**	**0.52**
Zn	**0.61**	**0.84**	**0.72**
Hg	0.22	0.08	0.23
Pb	0.13	0.05	**0.54**
As	0.00	0.01	0.31
Ba	0.23	**0.88**	**0.52**
Co	0.00	**0.40**	0.14
Cr	**0.64**	**0.82**	**0.57**
Ni	**0.28**	**0.78**	0.20
Sr	**0.58**	**0.57**	**0.41**

Values >0.26 exceed the 95% confidence level and are given in bold.

PCA of concentrations for well-leached elements for all cores confirmed the dominant role of [Al] in controlling down-core geochemical variability. For MWT-2 and MWT-6, the concentrations of half of the elements were predominantly explained by a single component (PC1), which related to [Al], confirming the need for normalization (Table 4). Other components did not account for much more than a single element, indicating no other major control on bulk geochemistry on a sample-by-sample comparison. When PCA was performed on the Al-normalized data to eliminate its effect, the cores showed some role for Fe and Mn binding, but neither was consistent across cores (Table 5). Overall, PCA provided an important test that demonstrates the only significant pattern among samples is the result of differential leaching as evidenced by [Al] differences. [Fe] differences were not found to explain differences in other elemental concentrations using PCA.

4.2. Down-core strata-averaged trends

Table 6 summarizes the distinct sequence of strata for each core including key variables from the precursor study by Brown and Pasternack (2004). When abundances of chemical constituents were averaged for each of the pre-defined strata, down-core differences were found to be strongly related to the type of strata

Table 3
Correlation matrix (R^2) for Al-normalized elements showing that few elements are inter-related in this setting once Al effects are accounted for

	Fe	Ca	Mg	Cu	Zn
(A) MWT-2					
Fe	X	0.44	0.22	0.20	0.30
Ca	X	X	0.12	0.05	0.24
Mg	X	X	X	0.24	**0.66**
Cu	X	X	X	X	0.38
Zn	X	X	X	X	X
(B) MWT-6					
Fe	X	0.00	**0.49**	0.27	0.37
Ca	X	X	0.07	0.03	0.00
Mg	X	X	X	0.19	0.19
Cu	X	X	X	X	0.06
Zn	X	X	X	X	X
(C) MWT-8					
Fe	X	0.00	0.10	0.14	0.10
Ca	X	X	0.04	0.21	0.14
Mg	X	X	X	0.07	**0.54**
Cu	X	X	X	X	0.09
Zn	X	X	X	X	X

rather than absolute depth (Figs. 5–7). Constituents such as Mn, P, Hg, As, Pb, S, and LOI varied significantly between strata, though not to an equal degree for all cores. Mn shows strongest variation between strata in MWT-6. Strong chemical stratification points to limited remobilization of elements, in addition to the evidence to this effect already described.

For MWT-2, the basal Pleistocene (>13,000 ybp) gray clay (MWT2-1) with high magnetic susceptibility had a distinct geochemical signature (Fig. 5). Even though its organic content was normal (i.e. 0–7% LOI), it had an extremely high concentration of S (3.1 ppt), whereas strata MWT2–6 only had 0.6 ppt S and other strata in MWT-2 had no detectible S. Associated with this S was a suite of higher concentration constituents, including Mn, Mg, Hg, Cu, Zn, and Ni. The origin of this layer is unknown and the radiocarbon date for it is beyond the calibrated range (Brown and Pasternack, 2004). The major sand channel unit in this core (MWT2-3) was notable for its relatively low [Hg] but high [As]. Distal floodplain fines (MWT2-4) showed an intermediate abundance of constituents. The surficial layer has experienced mixing due to agricultural plowing and it showed the highest LOI, [Al], [Hg] and [Pb] as well as the lowest [Fe], [Mg], and [Ni].

Core MWT-6 had alternating sand channel and distal floodplain strata with higher magnetic susceptibility and more charcoal fragments in lower strata. Many chemical constituents in this core showed little difference among strata, including Al, Fe, Mg, Cu, Zn, Ni, and Co (Fig. 6). The basal unit was a thick sand channel deposit that had relatively low LOI and [Mn]. Sand channel units showed lower LOI, [Al], [Mn], and [As] relative to distal floodplain strata. Conversely, they showed

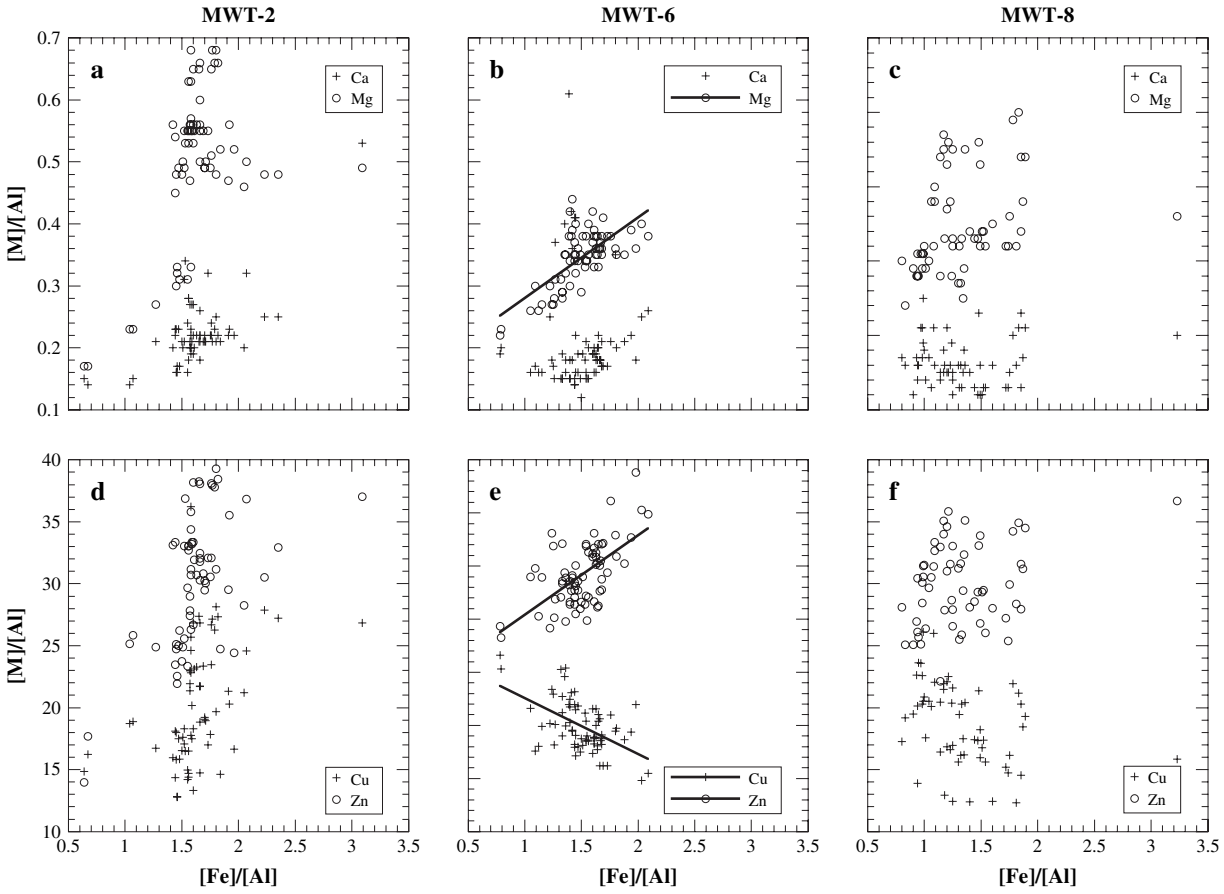

Fig. 4. Assessment of Fe-oxide control on element abundances after normalizing by Al.

Table 4
Principal components determined using raw concentrations of all well-leached elements

Variable	PC1	PC2	PC3	PC4	PC5
(A) MWT-2					
Al	**0.741**	0.018	−0.262	0.432	0.016
Fe	**0.884**	−0.124	0.181	0.115	0.046
Ca	**0.837**	−0.005	0.256	0.077	0.123
Mg	**0.924**	0.078	−0.054	−0.131	0.009
Mn	0.047	0.099	**0.906**	−0.059	0.019
S	−0.419	−0.458	0.112	−0.307	0.265
P	0.433	−0.101	0.352	0.588	0.009
Cu	**0.911**	0.056	−0.008	0.212	−0.052
Zn	**0.932**	0.170	−0.035	0.225	−0.037
Hg	0.008	0.196	−0.097	**0.878**	0.033
Pb	−0.074	0.010	0.014	−0.037	**−0.963**
As	−0.017	**−0.884**	−0.196	−0.157	0.014
Co	0.212	−0.620	0.536	0.138	−0.119
Ni	**0.901**	−0.161	0.249	−0.023	0.008
Variance	0.415	0.108	0.109	0.113	0.074
(B) MWT-6					
Al	**0.952**	−0.024	0.079		
Fe	**0.841**	0.145	0.168		
Ca	0.638	0.397	0.202		
Mg	**0.867**	0.230	0.162		
Mn	0.674	0.460	0.182		
S	−0.111	−0.594	−0.143		
P	0.207	**0.713**	−0.159		
Cu	**0.925**	−0.027	0.086		
Zn	**0.935**	0.091	−0.014		
Hg	−0.140	0.351	**−0.806**		
Pb	−0.305	0.545	−0.079		
As	0.100	0.417	0.692		
Co	**0.780**	−0.024	0.029		
Ni	**0.913**	−0.144	0.030		
Variance	0.470	0.138	0.095		
(C) MWT-8					
Al	0.508	0.313	0.657	0.239	
Fe	0.129	**0.905**	−0.019	−0.024	
Ca	0.378	0.143	**0.739**	−0.159	
Mg	**0.903**	0.140	0.129	−0.120	
Mn	0.071	0.666	0.690	0.024	
S	0.104	0.318	−0.413	**−0.725**	
P	0.054	**0.797**	0.343	−0.002	
Cu	0.574	−0.240	0.694	0.181	
Zn	**0.712**	0.339	0.551	0.069	
Hg	−0.156	0.499	0.651	−0.009	
Pb	0.186	0.122	**0.862**	0.087	
As	−0.164	−0.119	0.128	**−0.830**	
Co	0.583	0.130	0.027	0.341	
Ni	**0.901**	−0.136	0.185	0.037	
Variance	0.238	0.187	0.269	0.105	

Figures in bold type indicate high correlations between an element and a principle component. Last line of each section shows the fraction of the total variance explained by each component.

Table 5
Principal components determined using raw or Al-normalized concentrations as indicated

Variable	PC1	PC2	PC3	PC4	PC5
(A) MWT-2					
Al	−0.392	**0.835**	−0.124	0.050	0.035
S	0.253	−0.568	−0.241	0.387	0.159
P	0.277	**0.771**	0.066	0.007	0.104
Hg	−0.061	0.524	−0.450	−0.403	0.039
Pb	0.021	0.008	−0.026	−0.015	**−0.985**
As	−0.036	−0.093	−0.120	**0.919**	0.010
Fe/Al	**0.783**	−0.220	0.399	0.035	0.000
Ca/Al	**0.774**	−0.222	0.289	−0.124	0.100
Mg/Al	0.063	−0.105	**0.913**	−0.049	0.006
Mn	**0.867**	0.020	−0.041	−0.166	−0.032
Cu/Al	0.291	0.492	0.669	0.060	0.013
Zn/Al	0.303	0.065	**0.856**	−0.270	0.018
Co/Al	**0.783**	−0.077	0.113	0.337	−0.073
Ni/Al	0.678	0.004	0.603	0.142	0.040
Variance	0.242	0.201	0.195	0.096	0.070
(B) MWT-6					
Al	**0.876**	0.251	0.143	0.160	0.042
S	0.058	−0.565	0.259	0.000	−0.208
P	−0.007	**0.823**	0.184	−0.205	0.048
Hg	0.003	0.133	0.091	**−0.896**	−0.180
Pb	−0.229	−0.062	−0.204	−0.551	0.581
As	0.174	0.161	0.060	0.225	**0.731**
Fe/Al	**−0.848**	0.127	−0.324	0.019	−0.058
Ca/Al	0.003	0.354	0.089	−0.010	0.644
Mg/Al	**−0.795**	0.300	−0.145	−0.010	0.182
Mn	0.035	**0.800**	−0.142	0.046	0.173
Cu/Al	**0.783**	0.054	−0.262	0.107	0.246
Zn/Al	−0.476	0.159	−0.527	−0.331	0.031
Co/Al	−0.277	0.161	**−0.812**	0.077	−0.105
Ni/Al	0.606	−0.120	**−0.740**	0.053	0.020
Variance	0.292	0.137	0.125	0.091	0.100
(C) MWT-8					
Al	**0.842**	−0.190	0.326	−0.258	0.059
S	−0.343	0.152	−0.061	0.257	**0.801**
P	0.263	−0.141	**0.742**	−0.081	0.367
Hg	0.076	−0.091	**0.878**	0.032	−0.135
Pb	**0.710**	−0.177	0.471	0.026	−0.217
As	−0.164	0.088	0.065	**0.739**	0.044
Fe/Al	**−0.859**	0.130	0.107	0.161	0.133
Ca/Al	0.174	0.150	0.047	**0.859**	0.195
Mg/Al	−0.224	**0.771**	−0.273	0.209	0.303
Mn	−0.428	−0.054	**0.708**	0.427	−0.083
Cu/Al	0.548	0.453	−0.228	0.448	−0.375
Zn/Al	−0.145	**0.852**	0.148	0.229	0.231
Co/Al	−0.363	0.565	−0.101	−0.137	−0.307
Ni/Al	0.090	**0.930**	−0.185	0.063	−0.099
Variance	0.238	0.192	0.158	0.133	0.088

Figures in bold type indicate high correlations between an element and a principle component. Last line of each section shows the fraction of the total variance explained by each component.

higher [Fe] and associated magnetic susceptibility. Once again the agriculturally impacted surface layer (MT6-3c) showed significant enrichment in LOI and Hg as well as low [Fe] and [Mg].

Core MWT-8 was stratigraphically quite distinct from MWT-2 and MWT-6 in that it was predominantly composed of fine and organic sediment (Fig. 2), and this led to significant differences in geochemistry (Fig. 7). The basal clay unit in this core (MWT8-1) may have been deposited during either the late-Pleistocene or Holocene, and its [S] was below detection. It was enriched in Ni, Fe, Mg, and Ca, but had low [Al], [P], and [As]. The only sand unit in this core (MWT8-2) had high

Table 6
Strata present in the MWT cores (summarized from Brown and Pasternack, 2004)

Zone	Depth (cm)	Age (cal BP)	Vertical accretion rate (cm year^{-1})	Al (%)	Bulk density (g cm^{-3})	LOI	% Fines	Magnetic Susceptibility ($\times 10^{-5}$ SI units)	Charcoal (fragment cm^2 year^{-1})	Description
MWT2-6	0–100	0–800	0.12	3.1	1.7	5.9	94	16	0.3	Agriculture-impacted, tidally influenced upper deltaic plain
MWT2-5	100–230	800–2000	0.11	2	2.2	1.8	59	86	0.0	Tidally influenced transitional floodplain/delta with sand and fines
MWT2-4	230–430	2000–4000	0.10	2.4	2	3.4	77	53	0.0	Distal floodplain with fines
MWT2-3	430–1010	4000–13000	0.07	1.5	2.1	1.8	34	54	0.0	Sand channel unit with intermittent fines
MWT2-2	1010–1140	>13000	0.03	2.3	2	3.6	74	63	0.0	Pleistocene bands of green clay and silt
MWT2-1	1140–1325	>13000	n/a	2.4	1.7	4.8	97	178	0.0	Pleistocene gray clay
MWT6-3c	0–140	0–3800	0.04	2.7	1.9	8.3	94	15	0.0	Agriculture-impacted distal floodplain with fines; only tidally influenced in most recent period
MWT6-3b	140–260	3800–5500	0.07	2.1	1.9	4.6	63	15	0.1	Sand channel/bank unit
MWT6-3a	260–340	5500–6200	0.11	2.8	1.8	7.7	86	20	1.3	Distal floodplain with fines
MWT6-2b	340–520	6200–7500	0.14	1.8	2	2.7	25–69	152	0–16	Sand channel unit
MWT6-2a	520–700	7500–8500	0.21	2.8	1.9	4.8	58–85	152	0–1.2	Distal floodplain with fines
MWT6-1	700–1435	>8500	0.53	1.7	2.2	2	11–56	190–580	0–13	Sand channel unit
MWT8-5	0–90	0–700	0.12	3.2	1.8	6.4	90	63	1.0	Agriculture-impacted, tidally influenced upper deltaic plain
MWT8-4	90–480	700–4100	0.12	2.7	1.7	5.5	92	24	0.6	Tidally influenced upper deltaic plain
MWT8-3	480–850	4100–5400	0.30	3	1.4	6.1–32.1	95	10	0–54	Tidally influenced upper deltaic plain with peat-like wetland units
MWT8-2	850–1125	5400–6600	0.27	1.9	2.2	2	35	270	0–0.4	Sand channel unit with some gravel
MWT8-1	1125–1220	>6600	0.05	1.7	2	3.9	60	110	0.0	Green-blue clay

n/a, not available.

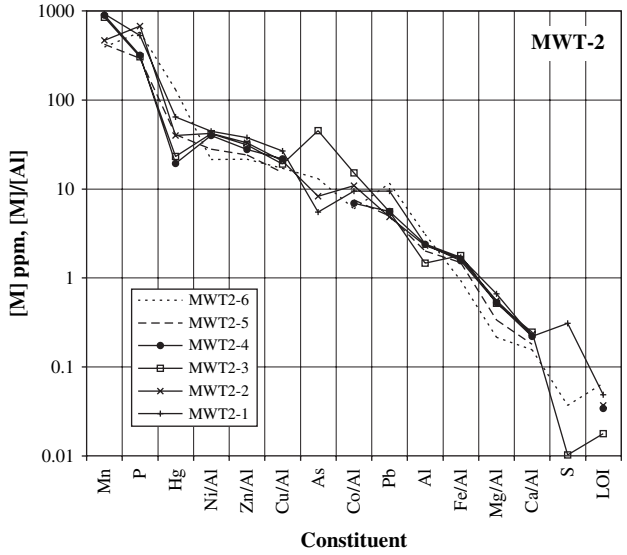

Fig. 5. Strata-averaged abundances of detectible elements in descending order for core MWT-2. Open symbols denote sand channel units, filled symbols denote fine floodplain and delta units, dotted line with no symbols denotes agriculture-impacted unit, dashed line with no symbols denotes a transitional unit, and stick symbols (+, ×) denote old clay units.

magnetic susceptibility but showed no enrichment and had low LOI and [Hg]. An organic-rich wetland strata in the middle of the core that dates to 4100–5400 cal BP (MWT8-3) was very high in LOI (up to 32%), S (2.1 ppt), and was rich in charcoal fragments. The surficial agricultural horizon was very highly enriched in Hg, P, Mn, and As and depleted in S.

4.3. Cross-core geochemical patterns

Cross-core strata-averaged abundances of elements showed distinct signatures for the four broad classes of strata (Fig. 8). Basal clays were high in S and associated metals that

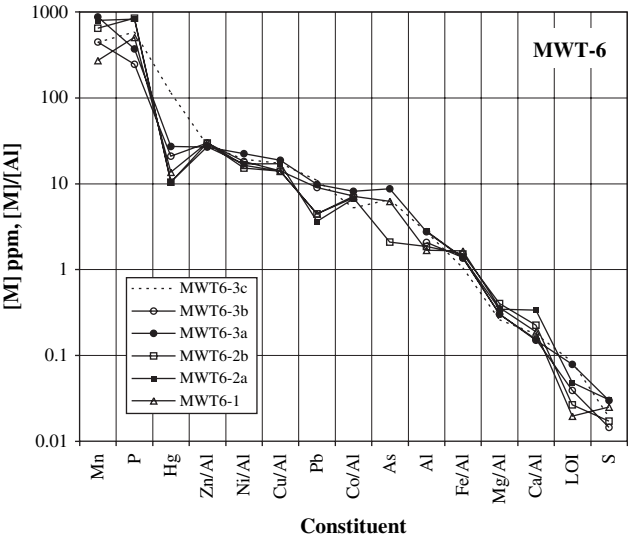

Fig. 6. Strata-averaged abundances of elements in descending order for core MWT-6. Symbols are the same as for Fig. 5.

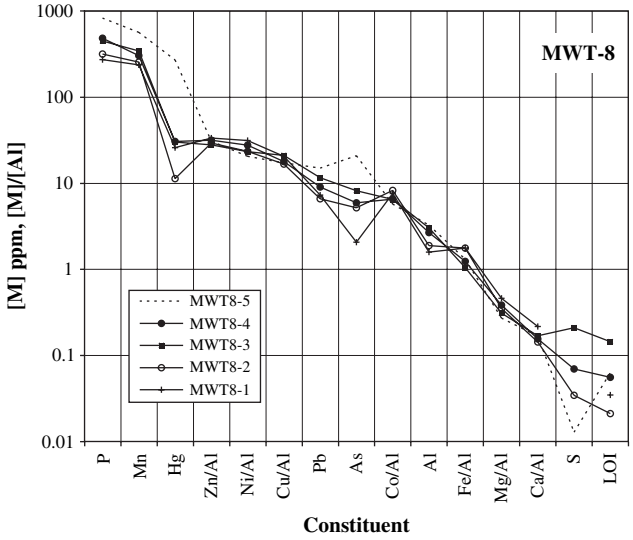

Fig. 7. Strata-averaged abundances of elements in descending order for core MWT-8. Symbols are the same as for Fig. 5.

precipitate in a reducing redox condition, including Fe, Mg, Ca, Zn, Cu, Ni. Sand channel units were relatively low in all chemical constituents except for Fe and As. The agriculturally impacted surface layer was highly enriched in Hg (4–11 times higher), and somewhat enriched in As, P, Co, Pb, and Al. It had the lowest [Fe], [Mg], and [Ca]. Distal floodplain units were intermediate in all constituent abundances.

Elemental abundances plotted as a function of time confirm that the cores showed very little synchronous geochemical fluctuation (Fig. 9). The elements whose abundances fluctuated most synchronously among cores were Hg and As. MWT-2 and -6 showed a dramatic increase in [Hg] from below 50 ppb to >200 ppb in the agriculturally disturbed layer, whereas MWT-8 peaked at 438 ppb in the same unit. This highly impacted horizon ranges from being 30 cm deep in MWT-2 to 120 cm in MWT-8. Because of mixing and surficial peat losses

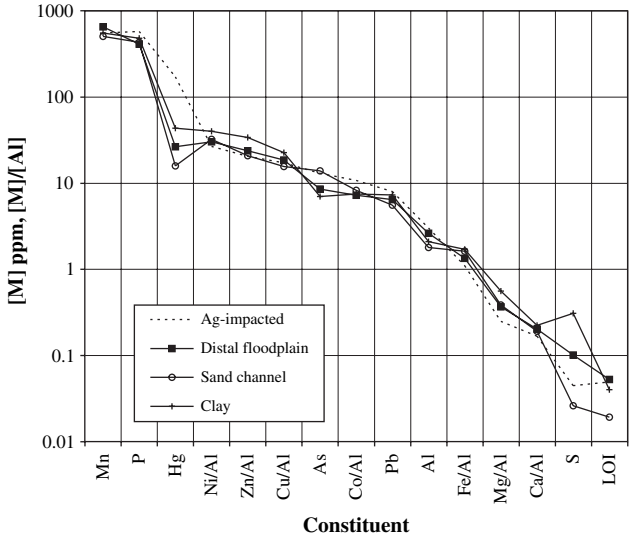

Fig. 8. Strata-averaged abundance of each elements in descending order averaged across all cores highlighting differences between endmembers.

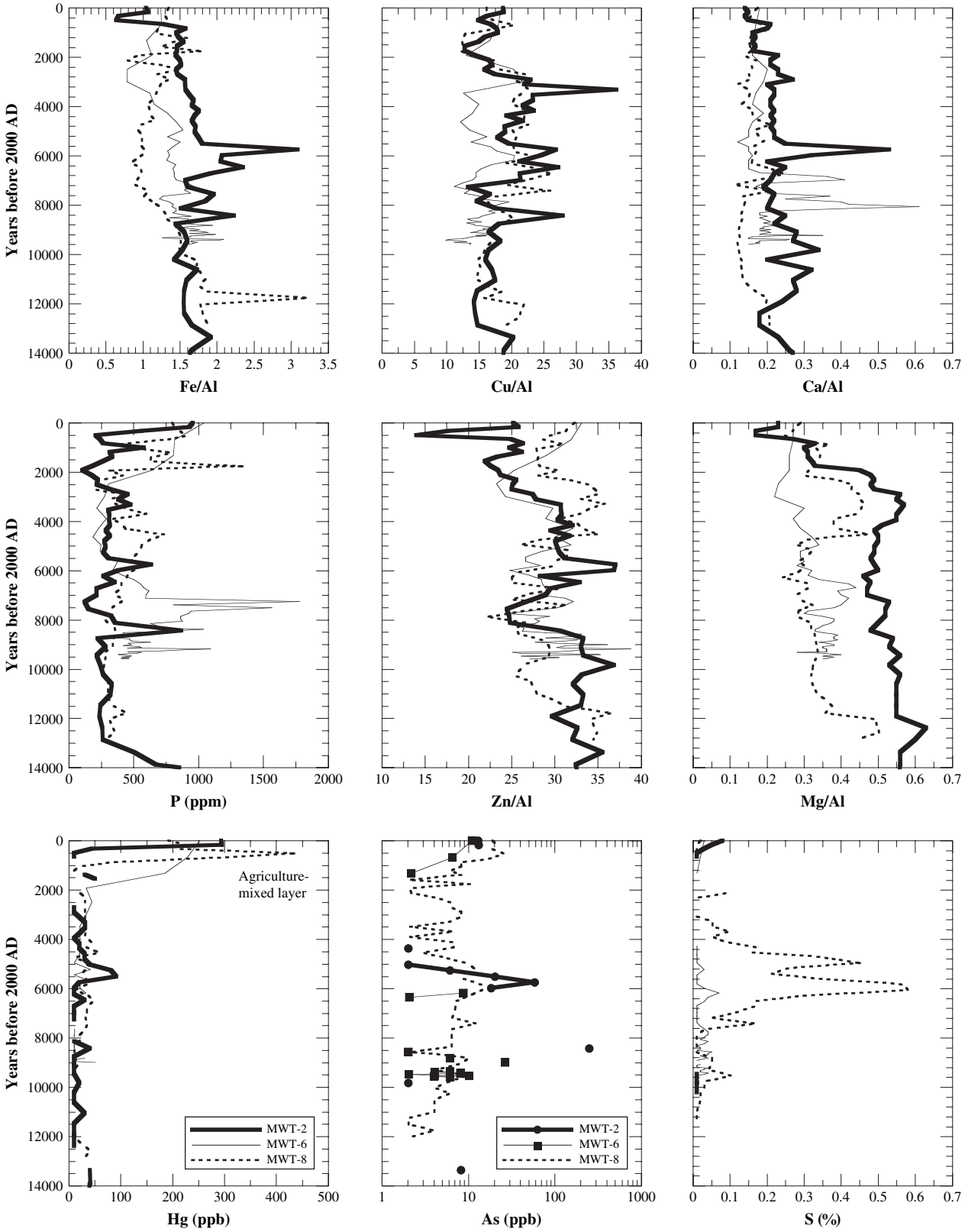

Fig. 9. Cross-core comparison of single element fluctuations through time.

via oxidation, the associated age of near-surface sediment in Fig. 9 is highly approximate and should not be used to suggest that the increase in Hg pre-dates human activity. According to the history recorded in the cores, [Hg] was at least 3 times lower throughout the past relative to its present concentration, implying that it is likely related to human activities. All cores also showed a higher abundance of [P] in the agriculturally impacted layer. MWT-6 had very high [P] and [Ca] in distal

floodplain fine sediments dating to 7000–8000 years ago. Arsenic was not detected in most strata, but there were some notable concentrations in the agricultural horizon and in ancient sand channel units. All cores showed an increase in [As] in the agricultural horizon, but not beyond prehistoric peaks, suggesting that As may have been naturally delivered to the site before settlement. MWT-2 had two [As] peaks in sand channel units and MWT-6 had a peak in [As] in one sand channel unit, further corroborating a natural source, with primary delivery occurring by floods.

Other elements had temporal fluctuations, and some of these clearly responded to stratigraphic controls (Fig. 9). For example, MWT-8 showed very high [S] in peaty layers mid-core. Also, [Mg] distinctly dropped in the topmost sections of MWT-2 and MWT-8. On the other hand, [Cu] and [Zn] showed frequent temporal fluctuations that did not reflect stratigraphy.

5. Discussion and conclusion

This was the first time that long sediment cores (12–14 m) collected on an upper deltaic plain have been assessed for their Holocene geochemical history. The three MWT cores analyzed in detail primarily showed typical bulk geochemical interrelationships (Loring, 1991; Knight and Pasternack, 2000). Careful assessment and adjustment for partial leaching effects enabled the comparison of different elements with different degrees of leaching. Aluminum extractability and grain-size distribution were found to act as master variables controlling first order geochemical dynamics. The results of the study provide the answers to the three questions posed in the introduction regarding geochemical remobilization, linkages between geomorphology and geochemistry, and the pollution trapping ability of upper deltaic plains.

5.1. Degree of remobilization

All cores were found to have low organic content. The only peaty deposits recovered in the cores were 4000–5000-year-old strata in MWT-8. This layer was also highly enriched in S. The lack of organic material generally among all cores demonstrates that the site was once non-tidal floodplain with predominantly basin-driven inorganic sediment accumulation associated with floods (Brown and Pasternack, 2004). Very little accumulation of in situ organic material occurred, whereas a lot of accumulation occurs in long-lived wetlands under reducing conditions. This conclusion clarifies that the upper deltaic plain was once a non-tidal floodplain that has been drowned by recent sea level rise.

The distributions of organic matter and S down-core provide circumstantial evidence about the prehistoric redox state of strata, which cannot be assessed by simply measuring Eh now. Wetland peats are associated with highly reducing conditions. If redox conditions permitted migration of constituents, then there would definitely be a difference between peaty and non-peaty layers. However, no elements other than S showed significant deviations in the peaty strata relative to the inorganic-dominated layers. This is good evidence that little mobilization and re-deposition of constituents has occurred in the sediments during the last 4000 years. Thus, the geochemistry of core strata are largely intact, so observed signatures can be confidently attributed to their original condition.

5.2. Geomorphic–geochemical linkages

Unlike typical wetland cores, those collected from MWT showed extremely different between-core geomorphic and geochemical conditions at any given time, indicative of strong spatial gradients and heterogeneity. This is a highly significant finding of this study with implications for the physical wetland restoration potential of upper deltaic plains. Deposits of the same type of strata were almost never synchronous between cores. Thus, rather than focusing on temporal variations typically associated with vertical accretion of wetlands, geochemistry was analyzed and interpreted in terms of strata-averaged conditions with a comparison of geochemistry within and between strata types. The MWT cores showed much less within-strata than between-strata variation in geochemistry. Almost all elements showed a preference for one strata type or another. For example, As was preferentially found in high concentrations in sand channel units and low concentrations in distal floodplain units, despite grain size effects.

Pleistocene deposits older than 11,500 years took the form of either chemically enriched clays or sand channel units. Since that time, MWT has been an alluvial floodplain. Major channels cut across the floodplain producing two endmember stratigraphic units: sand channel units and distal floodplain fine units. These units were found to be chemically distinct, with the channels relatively low in [Hg], [Al], [S], and LOI and high in [Fe], [As], and [Ni]. Each core showed an independent sequence of channels and distal floodplains, with each unit representing ~1000–2000 years. Because of this differential in local geomorphic process, the elevation and thus position relative to sea level of each core was very different. Drawing on the chronology of Brown and Pasternack (2004), MWT-8 was at sea level 6000–8000 years ago, most likely in a non-tidal, incised and abandoned channel. Strata MWT8-1 shows that at that time it developed S-enriched (~2.3 ppt) wetlands. It eventually came under tidal influence at ~1800 cal BP. In contrast, MWT-6 was well above sea level until very recently (~1000 cal BP). It had alternating sand and fine units with lower abundances of some elements in the sands and lower abundances of other elements in the fines (Table 6). MWT-2 was intermediate between MWT-6 and MWT-8 in its elevation, but also showed channel-distal floodplain banding and the associate geochemistry. MWT-2 became tidal at ~3000 cal BP.

5.3. Pollution retention

One factor common to all cores was the highly elevated Hg (4–11 times higher) and somewhat elevated As in the agriculturally impacted surface layer. The sources of Hg to the study area are Hg mines in the Coastal Range located northwest of

the delta. Hg was transported directly through surrounding streams such as Cache Creek and via its translocation and use in gold mining in the Sierra Nevada to the east. The sources for the somewhat elevated concentrations of Pb include industrial air pollution and car emissions. Arsenic comes from industrial combustion and high-temperature processes as well as insecticides, weed killers, fungicides, and wood preservatives. Phosphorus is derived primarily from agricultural and lawn fertilizers, transported downstream, and ultimately adsorbed onto sediment.

Because of plowing, the last 2000 years of sediment record has been mixed substantially, so the age-depth model cannot be specifically applied to detail this zone. Corn pollen—a distinct signature of agriculture that was not present before human agriculture in this area—was present throughout this zone, and proves that the observed peaks in the toxic elements Hg and As do not pre-date human intervention in the system. This does not imply that Hg derived from agriculture, but rather that it was stored during the agricultural era. The total abundance of Hg of ~200–400 ppb is significantly higher than that reported for Sacramento Valley sloughs and higher than that reported for most Sacramento-basin streambed sediment, except near the confluence with the Feather river, where oxidized sediments have [Hg] of 150–250 ppb (Domagalski, 2001). This suggests that under the typical reducing conditions expected after wetland restoration there would be a potential reactive-available concentration of up to 32 ppb. Since all cores showed highly elevated [Hg], inundation of the ~650 ha tract followed by tidal reworking would pose a significant post-restoration bioaccumulation hazard that needs to be addressed prior to any restoration.

Sediment quality guidelines have not been established in the United States, so the severity of the geochemical contamination hazard posed under current conditions cannot be assessed. Sediment bioassays are needed for this region prior to tidal restoration (Long and Chapman, 1985). Bioassays for sediments in delta tracts that were submerged after catastrophic levee failure or after pilot wetland restoration further downstream might provide insight into potential problems.

In many situations, P-availability limits growth of weedy aquatic plants in inland surface waters (NRC 1993). The critical concentration of P associated with accelerated weedy aquatic plant growth in marine and estuarine water is 0.001 mg kg^{-1} (Parry, 1998). Plants may also take up P from particulates. Thus, the observed doubling of [P] in the modern era significantly increases the likelihood of invasive weeds establishing when and if wetland restoration is performed. Due to the highly disturbed hydrogeomorphic condition associated with the flood regime post-restoration, this could be an important additional factor promoting the dominance of rapid-establishment pioneer weeds over slower growing native species.

Acknowledgements

The authors kindly thank The Seaver Institute, University of California, and CALFED (Ecosystem Restoration Program Co-op Agreement no. 114200J095) for providing funding for this research. We would like to thank Jeff Mount, Ken Verosub, Robert Zierenberg, Mike Singer, and Gary Weissmann for their discussions, comments, and resources. We thank The Nature Conservancy for access to their land, help in field logistics, and partnership in research, outreach, and education. We are grateful to Ellen Mantalica, Kaylene Keller, Derek Sappington, Mike Bezemek, Laurel Aroner, Wendy Trowbridge, Jim MacIntyre, Jose Constantine, and other volunteers for their assistance. Anonymous reviewers provided detailed comments that improved the manuscript.

References

Banus, M.D., Valiela, I., Teal, J.M., 1975. Lead, zinc, and cadmium budgets in experimentally enriched salt marsh ecosystems. Estuar. Coast. Mar. Sci. 3, 421–430.

Brown, K.J., Pasternack, G.B., 2004. The geomorphic dynamics of an upper deltaic floodplain tract in the Sacramento-San Joaquin Delta, California, USA. Earth Surf. Proc. Landf. 29, 1235–1258.

Cain, D.J., Carter, J.L., Fend, S.V., Luoma, S.N., Alpers, C.N., Taylor, H.E., 2000. Metal exposure in a benthic macroinvertebrate, *Hydropsyche californica*, related to mine drainage in the Sacramento River. Can. J. Fish. Aquat. Sci. 57, 380–390.

Choe, K.Y., Gill, G.A., Lehman, R., 2003. Distribution of particulate, colloidal, and dissolved mercury in San Francisco Bay estuary. 1. Total mercury. Limnol. Oceanogr. 48, 1535–1546.

Choi, M.H., Cech, J.J., Lagunas-Solar, M.C., 1998. Bioavailability of methylmercury to Sacramento blackfish (*Orthodon microlepidotus*): Dissolved organic carbon effects. Environ. Toxicol. Chem. 17, 695–701.

Colman, J.M., 1976. Deltas: Processes of Deposition and Models for Exploration. Continuing Education Publication Co., Champagne, IL.

Conomos, T.J., Peterson, D.H., 1976. Suspended-particle transport and circulation in San Francisco Bay: an overview. In: Wiley, M. (Ed.), Estuarine Processes, vol. 2: Circulation, Sediments, and Transfer of Materials in the Estuary. Academic Press, New York, pp. 82–97.

Domagalski, J., 1998. Occurrence and transport of total mercury and methyl mercury in the Sacramento River Basin, California. J. Geochem. Explor. 64, 277–291.

Domagalski, J., 2001. Mercury and methylmercury in water and sediment of the Sacramento River Basin, California. Appl. Geochem. 16, 1677–1691.

Dowdy, R.H., Larson, W.E., 1975. Metal uptake by barley seedlings grown on soils amended with sewage sludge. J. Environ. Qual. 4, 229–233.

Dubinski, B.J., Simpson, R.L., Good, R.E., 1986. The retention of heavy metals in sewage sludge applied to a freshwater tidal wetland. Estuaries 9, 102–111.

Elliot, T., 1986. Deltas. In: Reading,, H.G. (Ed.), Sedimentary Environments and Facies. Blackwell Scientific Publications, Oxford, pp. 113–154.

Florsheim, J.L., Mount, J.F., 2002. Restoration of floodplain topography by sand-splay complex formation in response to intentional levee breaches, Lower Cosumnes River, California. Geomorphology 44, 67–94.

Galloway, W.E., 1975. Process framework for describing the morphologic and stratigraphic evolution of deltaic depositional systems. In: Broussar, M.L. (Ed.), Deltas. Models for Exploration. Houston Geological Society, Houston, pp. 87–98.

Goodbred, S.L., Kuehl, S.A., 1998. Floodplain processes in the Bengal Basin and the storage of Ganges-Brahmaputra river sediment: an accretion study using ^{137}Cs and ^{210}Pb geochronology. Sed. Geol. 121, 239–258.

Hudson-Edwards, K.A., Macklin, M.G., Curtis, C.D., Vaughan, D.J., 1998. Chemical remobilization of contaminant metals within floodplain sediments in an incising river system: implications for dating and chemostratigraphy. Earth Surf. Proc. Landf. 23, 671–684.

Knight, M.A., Pasternack, G.B., 2000. Sources, input pathways, and distributions of Fe, Cu, and Zn in a Chesapeake Bay tidal freshwater marsh. Environ. Geol. 39, 1359–1371.

Logan, S.H., 1990. Global warming and the Sacramento-San Joaquin Delta. Calif. Agric. 44, 16–18.

Long, E.R., Chapman, P.M., 1985. A sediment quality triad: measures of sediment contamination, toxicity and infaunal community composition in Puget Sound. Mar. Poll. Bull. 16, 405–415.

Loring, D.H., 1991. Normalization of heavy-metal data from estuarine and coastal sediments. ICES J. Mar. Sci. 38, 101–115.

Millward, G.E., Moore, R.M., 1982. The adsorption of Cu, Mn, and Zn by Fe-oxyhydroxides in model estuarine solutions. Water Res. 16, 981–985.

Olsen, C.R., Cutshall, N.H., Larson, I.L., 1982. Pollutant-particle associations and dynamics in coastal marine environments: a review. Mar. Chem. 11, 501–533.

Olsenholler, S.M., 1991. Annual loading estimates of urban toxic pollutants in the Chesapeake Bay basin. Final report to USEPA, Chesapeake Bay Program, Metropolitan Washington Council of Governments, Washington.

Orson, R.A., Simpson, R.L., Good, R.E., 1992. A mechanism for the accumulation and retention of heavy metals in tidal freshwater marshes of the upper Delaware River estuary. Estuar. Coast. Shelf Sci. 34, 171–186.

Parry, R., 1998. Agricultural phosphorus and water quality: U. S. Environmental Protection Agency perspective. J. Environ. Qual. 27, 258–261.

Pasternack, G.B., 1998 Physical dynamics of tidal freshwater delta evolution. Ph.D. Thesis, Johns Hopkins University, Baltimore.

Pasternack, G.B., Hinnov, L.A., 2003. Hydro meteorological controls on water level in the upper reaches of a Chesapeake Bay tidal freshwater tributary. Estuar. Coast. Shelf Sci. 58, 373–393.

Pasternack, G.B., Brush, G.S., Hilgartner, W.B., 2001. Impact of Historic Land-Use Change on Sediment Delivery to a Chesapeake bay Subestuarine Delta. Earth Surf. Proc. Landf. 26, 409–427.

Rojstaczer, S.A., Hamon, R.E., Deverel, S.J., Massey, C.A., 1991. Evaluation of selected data to assess the causes of subsidence in the Sacramento-San Joaquin Delta, California. U.S. Geological Survey Open-File Report 91–193, 1–16.

Sculthorpe, C.D., 1967. The Biology of Aquatic Vascular Plants. Edward Arnold, London.

Simpson, R.L., Good, R.E., Dubinski, B.J., Pasquale, J.J., Philipp, K.R., 1983a. Fluxes of heavy metals in Delaware River freshwater tidal wetlands. Final Report. Center for Coastal and Environmental Studies. Rutgers University, New Brunswick.

Simpson, R.L., Good, R.E., Walker, R., Frasco, B.R., 1983b. The role of Delaware River freshwater tidal wetlands in the retention of nutrients and heavy metals. J. Environ. Qual. 12, 41–48.

United States Geological Survey, 1911. Topographical map of the Sacramento Valley, California. U.S. Geological Survey Atlas Sheets.

Varekamp, J.C., Pasternack, G.B., Rowe, G.L., 2000. Volcanic lake systematics II. Chemical constraints. J. Geother. Volcanol. Res. 97, 161–179.

Velinsky, D.J., Wade, T.L., Schlekat, C.E., McGee, B.I., Presley, B.J., 1994. Tidal river sediments in the Washington, D.C. area. I. distribution and sources of trace metals. Estuaries 17, 305–320.

Warren, L.J., 1981. Contamination of sediments by lead, zinc, and cadmium; a review. Environ. Pollut. (Ser. B) 2, 401–436.